THE AMERICAN SOCIETY OF MECHANICAL ENGINEERS
345 E. 47th St., New York, N.Y. 10017

97-GT-183

AN ANALYSIS METHOD FOR MULTISTAGE TRANSONIC TURBINES WITH COOLANT MASS FLOW ADDITION

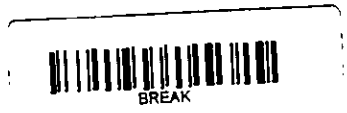

Frank Mildner and Heinz E. Gallus
Institut für Strahlantriebe und Turboarbeitsmaschinen
Rheinisch-Westfälische Technische Hochschule Aachen
Aachen, Germany

ABSTRACT

The subject of this paper is a numerical method for the calculation of the transonic flow field of multistage turbines taking high coolant flow into account. To reduce the processing time, a throughflow method based on the principels of Wu is used for the hub-to-tip calculation. The flow field is obtained by an iterative solution between a three dimensional inviscid hyperbolic time-dependent algorithm with an implicit finite volume method for the blade-to-blade calculations using C-meshes and a single representative meridional S_{2m}-stream surface. Along the S_{2m}-plane with respect to non-orthogonal curvilinear coordinates, the stream function equation governing fluid flow is established. The cooling air inflow inside the blade passage forbids the assumption of a constant mass flow along the main stream direction. To consider the change of the aerodynamic and thermodynamic behaviour, a cooling air model was developed and implemented in the algorithm, which allows the mixing of radially arbitrarily distributed cooling air in the trailing edge section of each blade row. The viscous effects and the influence of cooling air mixing are considered by the use of selected loss correlations for profile-, tip leakage, secondary flow and mixing losses in the S_{2m}-plane in terms of entropy. The method is applied to the four stage high temperature gas turbine Siemens KWU V84.3. The obtained numerical results are in good agreement with the experimental data.

NOMENCLATURE

$A_2, E_2, \bar{A}_2, \bar{F}_2$	Coefficients of the stream function equation
A	Area
$\hat{A}$, $\hat{B}$, $\hat{C}$	Flux-Jacobian-matrices
b	Stream sheet thickness
c	Dissipation constant
e	Energy per unit volume
$\hat{E}$, $\hat{F}$, $\hat{G}$	Flux vectors
f_k	Radial coolant distribution
h	Enthalpy
$\hat{H}$	Source vector
J	Jacobian
L, R	Left- and right sided Eigenvector matrices
Ma	Mach number
$\dot{m}$	Mass flow rate
p	static pressure
Q	Vector of dependent conservative variables
R	Gas constant
$\hat{s}$	Entropy
s, n	Curvilinear coordinates
t	time
T	Temperature
u	Circumferential velocity
u, v, w	Absolute cartesian velocities
w	Velocity
x, y, z	Cartesian coordinates
x, r, φ	Cylindrical coordinates
β	Relative flow angle
κ	Ratio of specific heat
Λ	Matrix of Eigenvalues
μ_1, μ_2	Stream surface gradients
μ	Numerical dissipation
ξ, η, ζ	Curvilinear coordinates
ρ, $\tilde{\rho}$	Density, artificial density
ψ	Stream function
Ω	Angular velocity

Subscripts

g	Gas
i	Inlet
k	Coolant
m	Meridional
rot	Rothalpy
t	Total
x, y, z	Partial derivative
x, r, u	Direction of velocity
1	Mixed out state

Presented at the International Gas Turbine & Aeroengine Congress & Exhibition
Orlando, Florida — June 2–June 5, 1997
This paper has been accepted for publication in the Transactions of the ASME
Discussion of it will be accepted at ASME Headquarters until September 30, 1997

Superscripts

^	Vector or matrix in transformed plane
l, r	Left- and right sided value resp.
ξ, η, ζ	Direction of velocity

INTRODUCTION

Continuous improvements in gas turbine development and thermodynamic cycle process are needed to conserve energy resources, cut back emissions and lower costs. To reach these goals, current development tend towards an increase of the turbine inlet temperature with a concurrent rise in the mass flow to increase the power/weight ratio of the machines. For this, the maximum power output and the overall thermal efficiency play major roles in the development of modern heavy duty high temperature gas turbines. The rise of the aerodynamic load of the blades in combination with the influence of modern cooling air configurations due to the high turbine inlet temperature hinder the aerodynamic design. Under these preconditions further improvement of the efficiency requires not only the investigation of single blade rows, but also the analysis of the flow field of complete transonic cooled turbomachine components.

In the early 1990s, several methods to calculate multistage turbomachinery components were developed which were based on solving the three dimensional Navier-Stokes equations (Ni and Bogoian, 1989, Dawes, 1990, Denton, 1990, Adamczyk et al., 1990, Chima, 1991, Hah et al., 1994, Arnone et al., 1994, 1995, Fan et al., 1995). Even taking into account the rapidly rising computer capacities, this is a very extensive and computer-time consuming method and still requires a long calculation time.

To reduce the processing time, throughflow methods are still in use, especially when, during the design process of a turbomachine, several calculations become necessary. The described numerical code is based on the publication of Wu (1951), in which he reduced the three dimensional flow problem into several two dimensional problems. In case of a pure subsonic flow pattern, the stream function equation can be solved with the finite difference method iteratively on S_1- (blade-to-blade) and one representative S_{2m}-plane (hub-to-tip) using non-orthogonal body fitted H-grids. In the case of transonic flow, especially when the flow is choked on several blade-to-blade planes, this procedure fails due to the non-uniqueness of the density in the stream function formulation. Therefore Wu's approach in the described code for S_1-planes is replaced by an inviscid hyperbolic algorithm with an implicit finite volume method using body fitted C-meshes (Benetschik et al., 1995). The interactive coupling of the three dimensional calculation of the single blade rows is performed on the S_{2m}-stream filament, which covers all blade rows of the turbomachine component. The S_{2m}-stream surface contains circumferentially averaged flow variables requiring that the S_1-planes are surfaces of revolution. The geometry of the S_{2m}-stream surface shape and the thickness are to be updated from the last cycle calculation on S_1-stream surface family.

Using the Artificial Compressibility Method (Hafez et al., 1978) on the S_{2m}-stream surface the discretization of the partial differential equation is carried out by use of the standard central difference formula and hence the procedure is greatly simplified. In order to overcome the non-uniqueness of density in transonic flow on S_{2m}-planes by use of the stream function equation, Hafez and Lowell (1981) proposed a technique. According to this method the velocities in the flow field are first obtained by integrating the momentum equation and then the density is determined by the energy equation.

Due to the results of a comparison of different loss correlations with a single stage Navier-Stokes calculation applied to the Siemens V84.3 (Mildner and Gallus, 1993), the correlation of Craig and Cox (1970) shows the best coincidence with the experimental data and is therefore integrated in the numerical code.

Effective turbine blade cooling is necessary to enhance the efficiency of gas turbines. Usually the coolant is mainly ejected through the trailing edge of the blades. In addition to the desired temperature reduction at the trailing edge, there is a three dimensional aerodynamic interaction between hot gas and the coolant. The complex mechanism of the mixture is a main problem in the numerical prediction of the flow field of cooled turbomachine components. The cooling air inflow inside the blade passage forbids the assumption of a constant mass flow and constant rothalpy along the main stream direction. While such phenomena are predictable with new Navier-Stokes solvers (Bohn et al., 1995, Michelassi et al., 1994) there is still a lack of methods when cooling air effects should be considered in Q3D-algorithms. Therefore, a cooling air mixing model will be presented within this paper which allows the mixing of radially distributed cooling air in the trailing edge section of each blade row.

HUB-TO-TIP CALCULATION

S_{2m}-STREAM FUNCTION EQUATION

Newton's 2nd Law of motion is initially cast into a cylindrical coordinate system rotating about the x-axis at an angular speed Ω. For a steady, adiabatic, inviscid flow the equation of motion reads as follows. Radial direction:

$$-\frac{w_u}{r}\left(\frac{\partial r w_u}{\partial r}-\frac{\partial w_r}{\partial \varphi}\right)+w_x\left(\frac{\partial w_r}{\partial x}-\frac{\partial w_x}{\partial r}\right)-2\Omega w_u=T\frac{\partial s}{\partial r}-\frac{\partial h_{rel}}{\partial r} \qquad (1)$$

circumferential direction:

$$-\frac{w_r}{r}\left(\frac{\partial r w_u}{\partial r}-\frac{\partial w_r}{\partial \varphi}\right)-w_x\left(\frac{\partial w_x}{r\partial \varphi}-\frac{\partial w_u}{\partial x}\right)+2\Omega w_r=\frac{T\,\partial s}{r\partial \varphi}-\frac{\partial h_{rel}}{r\partial \varphi} \qquad (2)$$

axial direction:

$$-w_r\left(\frac{\partial w_r}{\partial x}-\frac{\partial w_x}{\partial r}\right)+w_u\left(\frac{1}{r}\frac{\partial w_x}{\partial \varphi}-\frac{\partial w_u}{\partial x}\right)=T\frac{\partial s}{\partial x}-\frac{\partial h_{rel}}{\partial x} \qquad (3)$$

The stream surface shape can be described by $\varphi = \varphi(\bar{r}, \bar{x})$. The barred signs are used to denote, that a quantity q following the motion along S_{2m}-stream surface with respect to $\bar{x}$ and $\bar{r}$ lines on the meridional plane. The relations between these partial derivatives and ordinary spatial partial derivatives are given by:

$$\frac{\partial q}{\partial r} = \frac{\partial q}{\partial \bar{r}} + \frac{\mu_1}{r}\frac{\partial q}{\partial \varphi} \qquad (4)$$

$$\frac{\partial q}{\partial x} = \frac{\partial q}{\partial \bar{x}} + \frac{\mu_2}{r}\frac{\partial q}{\partial \varphi} \qquad (5)$$

where the stream surface gradients μ_1 and μ_2 are:

$$\mu_1 = -r\frac{\partial \varphi}{\partial \bar{r}} \qquad (6)$$

$$\mu_2 = -r\frac{\partial \varphi}{\partial \bar{x}} \tag{7}$$

A stream function equation can be introduced, which is obtained from the continuity equation for flow along a S_{2m}-stream surface

$$\frac{\partial \psi}{\partial \bar{x}} = -rb\rho w_r \tag{8}$$

$$\frac{\partial \psi}{\partial \bar{r}} = -rb\rho w_x \tag{9}$$

where b is the thickness of the stream filament. Using the condition that the circumferential velocity component has to follow the S_{1m}-stream surface

$$w_u = -\mu_1 w_r - \mu_2 w_x \tag{10}$$

the principel stream surface equation can then be obtained from Eqs. (1)-(10). By taking into account that the formulation is transformed into a non-orthogonal curvilinear s,n-coordinate system the formulation reads:

$$\bar{A}_2\frac{\partial^2\psi}{\partial \bar{s}^2} + \bar{B}_2\frac{\partial^2\psi}{\partial \bar{n}^2} + \bar{C}_2\frac{\partial^2\psi}{\partial \bar{n}\partial \bar{s}} + \bar{D}_2\frac{\partial\psi}{\partial \bar{s}} + \bar{E}_2\frac{\partial\psi}{\partial \bar{n}} = \bar{F}_2 \tag{11}$$

with the coefficients:

$$A_2 = \frac{1+\mu_1^2}{r} \tag{12}$$

$$B_2 = \frac{1+\mu_2^2}{r} \tag{13}$$

$$C_2 = -\frac{2\mu_1\mu_2}{r} \tag{14}$$

$$D_2 = \frac{1}{r}\left(\mu_1\frac{\partial \mu_1}{\partial \bar{x}} - \mu_2\frac{\partial \mu_1}{\partial \bar{r}}\right) \tag{15}$$

$$E_2 = \frac{1}{r}\left(\mu_2\frac{\partial \mu_2}{\partial \bar{r}} - \mu_1\frac{\partial \mu_2}{\partial \bar{x}} - \frac{1}{r}\right) \tag{16}$$

$$\bar{A}_2 = A_2\left(\frac{\partial s}{\partial \bar{x}}\right)^2 + B_2\left(\frac{\partial s}{\partial \bar{r}}\right)^2 + C_2\frac{\partial s}{\partial \bar{x}}\frac{\partial s}{\partial \bar{r}} \tag{17}$$

$$\bar{B}_2 = A_2\left(\frac{\partial n}{\partial \bar{x}}\right)^2 + B_2\left(\frac{\partial n}{\partial \bar{r}}\right)^2 + C_2\frac{\partial n}{\partial \bar{x}}\frac{\partial n}{\partial \bar{r}} \tag{18}$$

$$\bar{C}_2 = 2A_2\frac{\partial s}{\partial \bar{x}}\frac{\partial n}{\partial \bar{x}} + 2B_2\frac{\partial s}{\partial \bar{r}}\frac{\partial n}{\partial \bar{r}} + C_2\left(\frac{\partial n}{\partial \bar{x}}\frac{\partial s}{\partial \bar{r}} + \frac{\partial n}{\partial \bar{r}}\frac{\partial s}{\partial \bar{x}}\right) \tag{19}$$

$$\bar{D}_2 = A_2\frac{\partial^2 s}{\partial \bar{x}^2} + B_2\frac{\partial^2 s}{\partial \bar{r}^2} + C_2\frac{\partial^2 s}{\partial \bar{x}\partial \bar{r}} + D_2\frac{\partial s}{\partial \bar{x}} + E_2\frac{\partial s}{\partial \bar{r}} \tag{20}$$

$$\bar{E}_2 = A_2\frac{\partial^2 n}{\partial \bar{x}^2} + B_2\frac{\partial^2 n}{\partial \bar{r}^2} + C_2\frac{\partial^2 n}{\partial \bar{x}\partial \bar{r}} + D_2\frac{\partial n}{\partial \bar{x}} + E_2\frac{\partial n}{\partial \bar{r}} \tag{21}$$

$$\bar{F}_2 = \left[\frac{\partial s}{\partial \bar{r}}r\left(w_x B_2 - w_r\frac{C_2}{2}\right) - \frac{\partial s}{\partial \bar{x}}r\left(w_r A_2 - w_x\frac{C_2}{2}\right)\right]\frac{\partial b\rho}{\partial s} + \left[\frac{\partial n}{\partial \bar{r}}r\left(w_x B_2 - w_r\frac{C_2}{2}\right) - \frac{\partial n}{\partial \bar{x}}r\left(w_r A_2 - w_x\frac{C_2}{2}\right)\right]\frac{\partial b\rho}{\partial n} - \left[\frac{1}{w_x}\left(T\left(\frac{\partial s}{\partial \bar{r}}\frac{\partial \hat{s}}{\partial s} + \frac{\partial n}{\partial \bar{r}}\frac{\partial \hat{s}}{\partial n}\right) - \left(\frac{\partial s}{\partial \bar{r}}\frac{\partial h_{rot}}{\partial s} + \frac{\partial n}{\partial \bar{r}}\frac{\partial h_{rot}}{\partial n}\right)\right) + 2\mu_2\Omega\right]b\rho \tag{22}$$

MESH GENERATION

As the equation to be solved is expressed with respect to a non-orthogonal curvilinear coordinate system, the discretization can be done directly on a arbitrary type mesh. In the present calculation a body fitted H-type mesh was used. Figure 1 shows an example for a two stage gas turbine with 143 x 25 grid nodes. To consider strong flow variable gradients due to the implemented loss- and cooling air mixing model, mesh refining near hub and shroud is utilized.

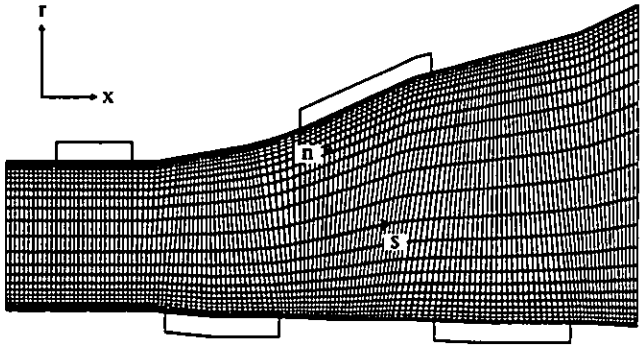

Fig. 1: Non-orthogonal coordinates and computational grid

DETERMINATION OF DENSITY

In the stream function formulation the density is not a unique function of the mass flux, and for subsonic flow the density is updated by using the following iteration procedure, where the entropy is taken into account in the density calculation:

$$\rho_{NEW} = \rho_i\left[\frac{h_{rot} + \frac{1}{2}\Omega^2 r^2 - \frac{\frac{1}{2}(\rho w)^2}{\rho^2_{OLD}}}{h_i}\right]^{\frac{1}{\kappa-1}} e^{(s_i - s)} \tag{23}$$

To calculate the density in mixed flow domains, Eq. (1) is rewritten as a velocity gradient equation:

$$w_{x_{i,j+1}}^{NEW} = w_{x_{i,j}}^{NEW} + \int_{r_{i,j}}^{r_{i,j+1}}\left[\frac{\partial w_r}{\partial \bar{x}} + \mu_2\left(\frac{w_u}{r} + \frac{\partial w_u}{\partial \bar{r}} + 2\Omega\right) - \mu_1\frac{\partial w_u}{\partial \bar{x}} - \frac{1}{w_x^{OLD}}\left(T\frac{\partial \hat{s}}{\partial \bar{r}} - \frac{\partial h_{rot}}{\partial \bar{r}}\right)\right]dr \tag{24}$$

The terms on the right hand side are updated consistently with the main calculation of ψ. The distribution of w_x from hub to shroud may be determined by integrating Eq. (24) along the radial direction after transformation into the s,n-coordinate system. The integration procedure proceeds from an assumed value of w_x on an initial data curve. Since the supersonic flow

regions of the circumferential averaged S_{2m}-flow normally do not extend to the hub for rotors and to the casing for stators in case of transonic turbines, the integration direction can be selected as shown in Fig. 2. Along an initial data curve near hub or shroud, where the flow is subsonic, the distribution of ρ and w_x along the corresponding curve may be obtained by use of Eq. (23) like in subsonic flow.

After integration w_r is updated from

$$w_r = w_x \frac{\frac{\partial \psi}{\partial x}}{\frac{\partial \psi}{\partial r}} \tag{25}$$

After knowing w_x and w_r, the density ρ can then obtained from Eq. (23).

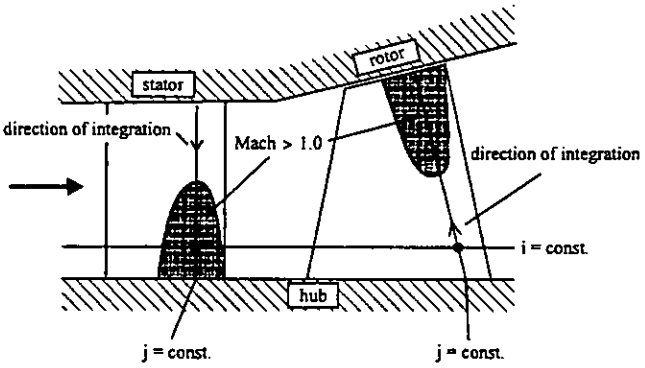

Fig. 2: Location of transonic regions

Since Eq. (11) is of mixed type in the transonic regime, the artificial density is introduced to ensure the stability of the computation in the supersonic regions. This method consists of modifying the density so as to introduce numerical dissipation. The modified density $\tilde{\rho}$ is obtained as follows:

$$\tilde{\rho} = \rho - \mu \frac{\partial \rho}{\partial s} \Delta s \qquad \mu = \max\left[0,\ c\left(1 - \frac{1}{Ma^2}\right)\right] \tag{26}$$

where c is ranging from 1.5 to 2. The discretization scheme for the density at grid point (i,j) takes the form:

$$\tilde{\rho}_{i,j} = \rho_{i,j} - \mu_{i,j}\left(\frac{w_x}{w_m}(\rho_{i,j} - \rho_{i-1,j}) + \frac{w_r}{w_m}(\rho_{i,j} - \rho_{i,j-1})\right) \quad [w_r > 0] \tag{27}$$

$$\tilde{\rho}_{i,j} = \rho_{i,j} - \mu_{i,j}\left(\frac{w_x}{w_m}(\rho_{i,j} - \rho_{i-1,j}) + \frac{w_r}{w_m}(\rho_{i,j+1} - \rho_{i,j})\right) \quad [w_r < 0] \tag{28}$$

BOUNDARY CONDITIONS AND SOLUTION METHOD

The boundary conditions of flow along the S_{2m}-stream surface should be specified. At the inlet boundary the stagnation pressure, stagnation temperature and the mass flow rate are given. At the solid walls, the stream function value should be equal to zero (at hub), or $\dot{m}$ (at shroud). At the outlet boundary, the relative flow angle is given.

Standard finite discretizing Eq. (11) leads to a large system of nonlinear algebraic equations in the unknown stream function values at the grid points in the form:

$$|A|\ \Psi = \bar{B} \tag{29}$$

The coefficient matrix A contains only metric quantities and remains unchanged, while the right hand side contains the density $\tilde{\rho}$, the independent thermodynamic properties entropy $\hat{s}$ and the stagnation rothalpy h_{rot} and must be updated during the iteration process. Together with the discretized boundary conditions, the formulation of the discrete problem is complete, and a direct matrix method is utilized to solve the nonlinear algebraic equation.

BLADE-TO-BLADE CALCULATION

GOVERNING EQUATIONS

The three dimensional, compressible, inviscid and unsteady flow is described by the Euler equations. For the correct computation of the propagation speed and the intensity of discontinuities, a conservative formulation in a rotating cartesian frame of reference is used. Transformed into a general curvilinear system the Euler equations are defined as follows:

$$J\frac{\partial Q}{\partial t} + \frac{\partial \hat{E}}{\partial \xi} + \frac{\partial \hat{F}}{\partial \eta} + \frac{\partial \hat{G}}{\partial \zeta} = \hat{H} \tag{30}$$

where the state vector Q comprising the conserved quantities, $\hat{E}$ $\hat{F}$, $\hat{G}$ are the Euler fluxes and $\hat{H}$ describes the source term:

$$Q = \begin{pmatrix} \rho \\ \rho u \\ \rho v \\ \rho w \\ e_{rot} \end{pmatrix} \quad \hat{E} = J\begin{pmatrix} \rho w^{\xi} \\ \rho u w^{\xi} + p\xi_x \\ \rho v w^{\xi} + p\xi_y \\ \rho w w^{\xi} + p\xi_z \\ w^{\xi}(e_{rot} + p) \end{pmatrix} \quad \hat{F} = J\begin{pmatrix} \rho w^{\eta} \\ \rho u w^{\eta} + p\eta_x \\ \rho v w^{\eta} + p\eta_y \\ \rho w w^{\eta} + p\eta_z \\ w^{\eta}(e_{rot} + p) \end{pmatrix} \tag{31}$$

$$\hat{G} = J\begin{pmatrix} \rho w^{\zeta} \\ \rho u w^{\zeta} + p\zeta_x \\ \rho v w^{\zeta} + p\zeta_y \\ \rho w w^{\zeta} + p\zeta_z \\ w^{\zeta}(e_{rot} + p) \end{pmatrix} \quad \hat{H} = J\begin{pmatrix} 0 \\ 0 \\ \rho w\Omega \\ -\rho v\Omega \\ 0 \\ 0 \end{pmatrix}$$

This set is closed by the assumption of a perfect gas:

$$e_{rot} = \frac{p}{\kappa - 1} + \frac{\rho}{2}(u^2 + v^2 + w^2) - \rho\Omega(yw - zv) \tag{32}$$

The Jacobian J represents the volume of the discretization element. In these equations u, v, w denote the absolute cartesian velocities. The contravariant relative transport velocities are given by:

$$\begin{aligned} w^{\xi} &= u\xi_x + (v + \Omega z)\xi_y + (w - \Omega y)\xi_z \\ w^{\eta} &= u\eta_x + (v + \Omega z)\eta_y + (w - \Omega y)\eta_z \\ w^{\zeta} &= u\zeta_x + (v + \Omega z)\zeta_y + (w - \Omega y)\zeta_z \end{aligned} \tag{33}$$

To solve the Euler equations, a quasi-conservative formulation is used. This formulation results from the Euler equations by

exchanging the fluxes by products of the flux-Jacobian-matrices and the spatial derivatives of the vector of dependent variables:

$$\frac{\partial \hat{Q}}{\partial t} + \hat{A}\frac{\partial \hat{Q}}{\partial \xi} + \hat{B}\frac{\partial \hat{Q}}{\partial \eta} + \hat{C}\frac{\partial \hat{Q}}{\partial \zeta} = \hat{H} \tag{34}$$

with the flux-Jacobian-matrices following from:

$$\hat{A} = \frac{\partial \hat{E}}{\partial \hat{Q}} \quad , \quad \hat{B} = \frac{\partial \hat{F}}{\partial \hat{Q}} \quad , \quad \hat{C} = \frac{\partial \hat{G}}{\partial \hat{Q}} \tag{35}$$

NUMERICAL ALGORITHM

The numerical solution follows a Godunov-type upwind scheme, fomulated in node centered finite volume technique using body fitted C-meshes. Assuming initial states Q^r to the right and Q^l to the left of each finite volume cell face being defined, fluxes are computed using Roe's approximate Riemann solver (Roe, 1981). Across a cell face $\xi_{i+1/2,j,k}$ the numerical flux function reads:

$$\hat{E}_{i+1/2,j,k} = \frac{1}{2}\left[\hat{E}(Q^l_{i+1/2,j,k}) + \hat{E}(Q^r_{i+1/2,j,k}) - \hat{R}^{\xi}|\hat{\Lambda}^{\xi}|\hat{L}^{\xi}(Q^r_{i+1/2,j,k} - Q^l_{i+1/2,j,k})\right] \tag{36}$$

where $\hat{R}^{\xi}$, $\hat{L}^{\xi}$ and Λ^{ξ} are the matrices of right and left Eigenvectors and the diagonal Eigenvalue matrix with respect to the Jacobian matrix of the inviscid flux vector.

The described scheme is only first order accurate. To reduce the diffusive character of first order schemes and to obtain a high resolution result an extension to higher order has to be made. This is possible by replacing the piecewise constant data in the discretization cells by linear varying initial data (van Leer, 1979) and leads to the MUSCL technique (Monotonic Upstream Schemes for Conservation Laws). A third order accuracy can be achieved with this technique. The flux-functions are still evaluated using only right and left states, but these states are second or third order accurate in space.

The disadvantage of a higher order scheme is its liability to oscillations in case of a discontinuous solution. To prevent this, a switch is needed, which reduces the extrapolation to first order in such regions. The scheme mostly used is the TVD-scheme (Total Variation Diminishing, Harten, 1983). It contains a limiter function based on sensors for strong changes in the flow values and reduces the order of extrapolation in these regions. A differentiable flux-limiter function following van Albada was chosen here, which is a compromise between the claim on stability and the claim on smooth extrema.

The solution is advanced implicitly in time using the delta-form:

$$\left(\frac{JE}{\Delta t} + \frac{\Delta_\xi \hat{A}^- + \nabla_\xi \hat{A}^+}{\Delta \xi} + \frac{\Delta_\eta \hat{B}^- + \nabla_\eta \hat{B}^+}{\Delta \eta} + \frac{\Delta_\zeta \hat{C}^- + \nabla_\zeta \hat{C}^+}{\Delta \zeta} - \frac{\partial \hat{H}_{i,j,k}}{\partial Q}\right)^n \Delta Q = -\left(\frac{\hat{E}_{i+1/2,j,k} - \hat{E}_{i-1/2,j,k}}{\Delta \xi} + \frac{\hat{F}_{i,j+1/2,k} - \hat{F}_{i,j-1/2,k}}{\Delta \eta} + \frac{\hat{G}_{i,j,k+1/2} - \hat{G}_{i,j,k-1/2}}{\Delta \zeta} - \hat{H}_{i,j,k}\right)^n \tag{37}$$

where $\hat{A}^{\pm}$, $\hat{B}^{\pm}$and $\hat{C}^{\pm}$ are the 5x5 Jacobians of the inviscid fluxes, which are computed from Roe's scheme first order of accuracy. To avoid excessive computational complexity, the Roe matrices, e.g. with respect to a cell face ξ=const. $\hat{R}^{\xi}|\hat{\Lambda}^{\xi}|\hat{L}^{\xi}$ are not linearized in time.

BOUNDARY TREATMENT

For a correct physical formulation of the boundary conditions, the method of characteristics is used. If the Eigenvectors of the characteristic equations run out of the computational domain, they have to be replaced by explicit boundary conditions. The added conditions are upstream total temperature, total pressure, inflow angle and downstream static pressure. Due to the fact, that the Euler algorithm is embedded into the multistage calculation procedure, the downstream boundary condition has to satisfy the conservation of mass of the turbomachine component. For that, the static pressure in combination with the radial equilibrium between the radial stream sheets in the axial gap is updated during the iteration procedure. For supersonic upstream or downstream conditions, the influence of the corresponding prescribed values is modified. On the profile the slip condition for inviscid flow is utilized, which means, that the flow is tangent to the blade and the component of the flow velocities normal to the blade is equal to zero.

COUPLING OF THE FLOW SOLVERS

The coupling of the stream function solver on S_{2m}-stream surface and the Euler algorithm is shown in Fig. 3.

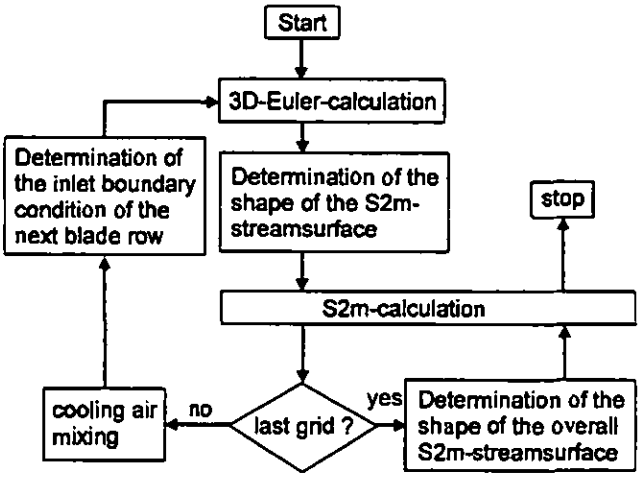

Fig. 3: Flowchart of the Q3DM-algorithm

In a first step, each blade row is calculated with the Euler algorithm to provide the thickness b and the stream surface gradients μ_1 and μ_2 of the stream surface of the individual blade row. The circumferential coordinate φ of the S_{2m}-stream surface results from the circumferentially mass averaged primitive variables of the Euler solution:

$$\tan\varphi = \frac{\int_{pitch}\left(\frac{1}{\sqrt{y^2+z^2}}(vz - wy) + \Omega\sqrt{y^2+z^2}\right) d\dot{m}}{\int_{pitch} u \, d\dot{m}} \tag{38}$$

After knowing the circumferential coordinate φ, the S_{2m}-stream surface gradients μ_1 and μ_2 are determined by finite differences. The S_{2m}-stream sheet thickness b results from the blockage of the blade profils and reads:

$$b = \frac{pitch - blade\ thickness}{pitch} \tag{39}$$

Subsequently the S_{2m}-stream solver is utilized. Considering the mixing of the cooling air and the losses described by the implemented loss model, the solution provides a realistic inflow boundary condition to the next blade row. In this manner each blade row is handled until the last one is reached. In a final step the interaction between the single blade rows takes place by calculating the whole turbomachine component with an overlapping S_{2m}-solution of all blade rows.

COOLING AIR MIXING

MATHEMATICAL MODEL

The mixing of cooling air with the main flow can be described by the conservation of mass, momentum and energy of a perfect gas:

$$\frac{w_{x,1}\,\rho_1\,A_1}{\dot{m}_1} - 1 = 0 \tag{40}$$

$$\dot{m}_1 w_{x,1} - w_{x,g}(\dot{m}_g + C_2\dot{m}_k) + p_1 A_1 - p_g(A_g + C_1 C_3 A_1) = 0 \tag{41}$$

$$\frac{T_1}{T_{t,1}} + \frac{(\kappa - 1)\left(w_{x,1}^2 + w_{r,1}^2 + (w_{x,1}\tan(\beta_1) + u_1)^2\right)}{2\,\kappa\,R\,T_{t,1}} - 1 = 0 \tag{42}$$

$$\frac{p_1}{\rho_1} - RT_1 = 0 \tag{43}$$

In these equations it is assumed, that the coolant is mainly ejected through the trailing edge of the blades and the mixing takes place at a constant static pressure. Moreover it is assumed, that the coolant is ejected in the direction of the main gas flow, and does not influence the deviation. The index I denotes the totally mixed out state downstream of the mixing area, whose axial extension is supposed to be small. The index g stands for the main gas flow quantities, while the index k describes the coolant.

The set of equations is triple undetermined and can be closed by the definition of the constants C_1 to C_3:

$$C_1 = \frac{A_k}{A_1} \qquad C_2 = \frac{w_{x,k}}{w_{x,g}} \qquad C_3 = \frac{p_k}{p_g} \tag{44}$$

While C_1 depends only on geometry, C_2 and C_3 are assumptions based on empirical data and have to be updated during the design process. The solution of this set of equations is found by applying a Newton-Raphson iteration where the given variable combination $(\dot{m}_1, T_{t,1}, w_{x,1}/w_{u,1}, w_{x,1}/w_{r,1})$ is transformed into the state vector of the mixed out quantities $(w_{x,1}, \rho_1, T_1, p_1)^T$.

NUMERICAL ALGORITHM

Due to the assumption, that the axial extension of the mixing area is small, numerically, the mixing takes place in a mixing

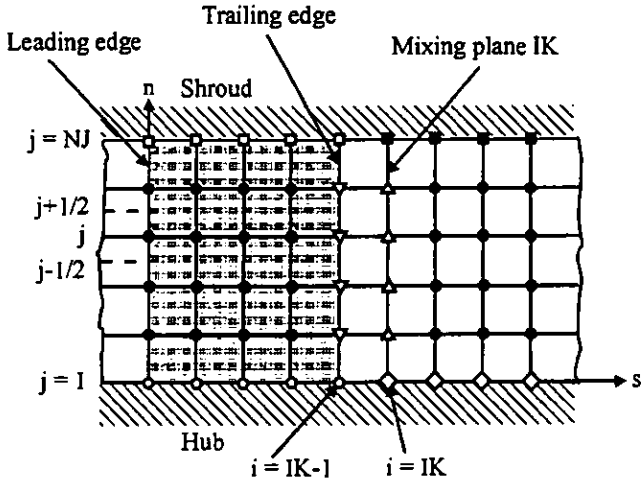

Fig. 4: Schematic section of the computational grid of the S_{2m}-stream surface

plane *IK* downstream of the trailing edge shown in Fig. 4. This yields to a jump in terms of mass, momentum and energy and influences the dependent variable ψ. For this, additional jump conditions have to be introduced. The different signs at the grid nodes in Fig. 4 represent the varying boundary and mixing conditions in the computational domain described as follows. Upstream the mixing plane ψ is given by:

- ○ $\psi_{i,1} = const.$
- □ $\psi_{i,NJ} = \psi_{i,1} + \dot{m}_g / 2\pi$

Downstream the mixing plane the boundary conditions define the grown mass flux:

- ◇ $\psi_{IK,1} = \psi_{IK-1,1} - \dot{m}_k / 4\pi$
- ■ $\psi_{IK,NJ} = \psi_{IK-1,NJ} + \dot{m}_k / 4\pi$

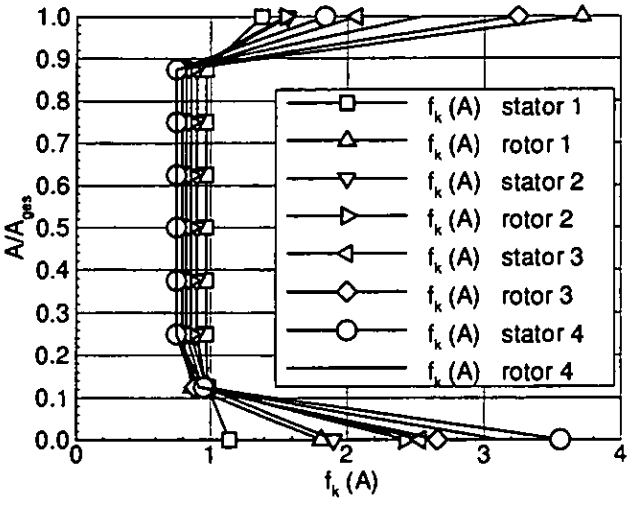

Fig. 5: Radial distribution of the cooling air of the V84.3

To consider the convective transport mechanisms across the mixing plane the calculation of the stream function at the △-nodes takes place by integration of the continuity equation in the radial direction:

$$\psi_{IKJ} = \psi_{IKJ-1} + \psi_{IK-1J} - \psi_{IK-1J-1} + \dot{m}_k \int_{\left(\frac{A}{A_{ges}}\right)_{j-1/2}}^{\left(\frac{A}{A_{ges}}\right)_{j+1/2}} f_k(A)\, d\left(\frac{A}{A_{ges}}\right) \qquad (45)$$

where the function f_t describes the radial distribution of the cooling air. Figure 5 shows the implemented distribution for the calculated Siemens gas turbine. Due to the jump of the density in the mixing plane, Eq. (11) is not steadily differentiable across the mixing plane. Therefore all ∇-nodes were discretized in upstream direction with first order in space, while the Δ-nodes were discretized in downstream direction with first order in space. All $\bullet$-nodes are approximated with a central differential scheme.

RESULTS

For validation of the developed code, called **Q3DM**, the Siemens gas turbine V84.3 has been investigated. At design conditions, the mass flow is 417 kg/s at a rotation rate of 3600 rpm. Due to the high turbine inlet temperature, the first seven of the eight blade rows in the four-stage turbine are cooled, whereby an intercooler is provided for more effective blade cooling in the first turbine stage. Figure 6 illustrates a cross-section of the described turbine. Referring to Fig. 6, it can be seen that the rotating blades in the first stage are shrouded in order to reduce the tip losses. The proven combination of convection and impingement was selected as the cooling method.

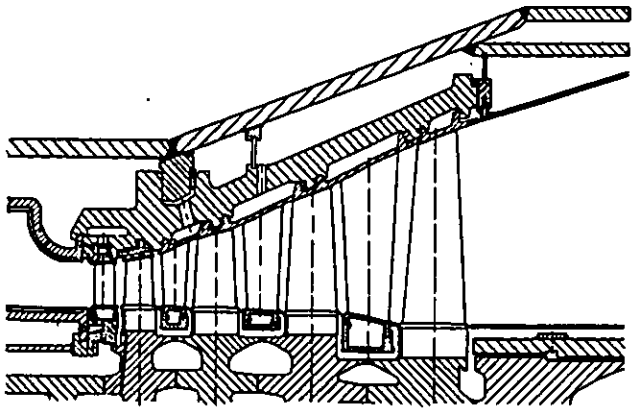

Fig. 6: Cross-section of gas turbine V84.3

Figure 7 to 9 show the results of the three dimensional Euler calculation. As expected, the Mach number level increases from turbine inlet to turbine outlet. While the Mach number distribution remains below the critical value in the first blade row (Fig. 7), choked flow can be found at the turbine exit (Fig. 8). The contour plot of the Mach number at midspan in Fig. 9 gives a survey of the location of the shock. In order to reduce the overall CPU time, a coarse computational mesh (9x65x9 grid nodes) was selected, which causes a non sharp resolution of the shock. Since the result of the Euler calculation is circumferentially averaged to generate the thickness and the shape of the S_{2m}-stream surface, it has been shown, that the resolution of the computational domain is sufficient. For brevity, a more detailed documentation of the inviscid solution is omitted here.

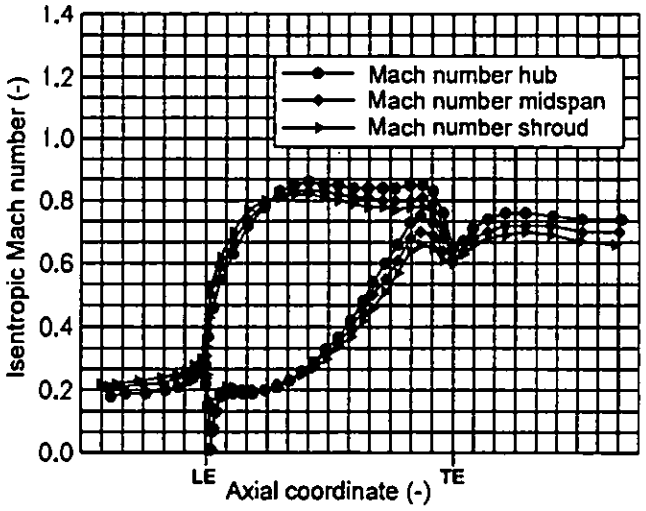

Fig. 7: Isentropic Mach number distribution, blade row 1

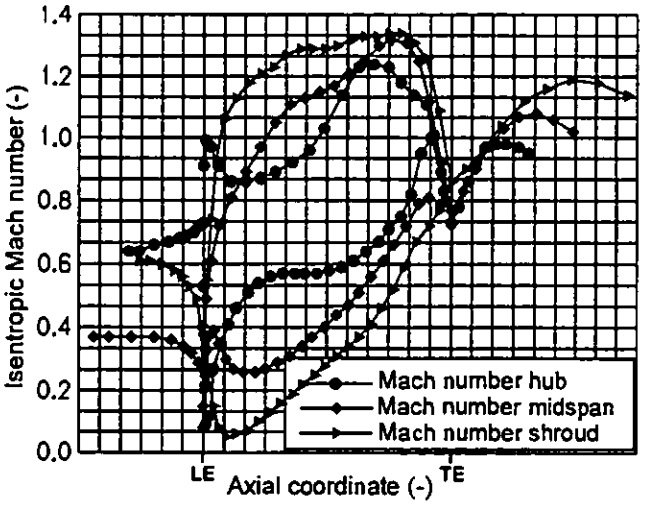

Fig. 8: Isentropic mach number distribution, blade row 8

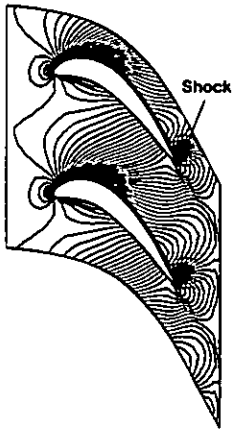

Fig. 9: Mach contour 8. blade row (midspan)

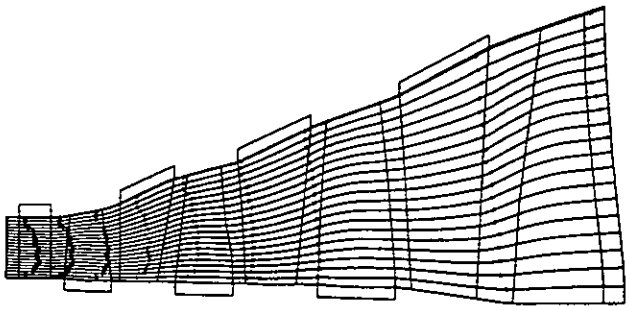

Fig. 10: Computed streamlines on S_{2m}-stream surface

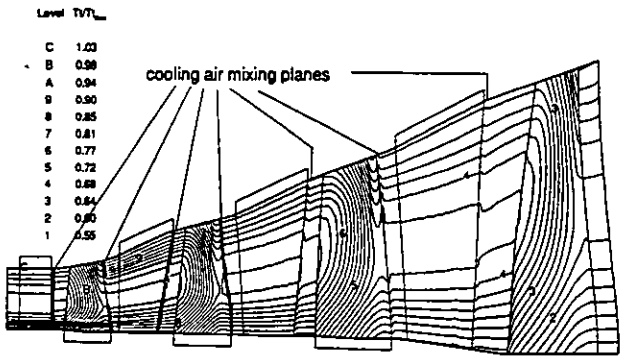

Fig. 11: Computed total temperature contour

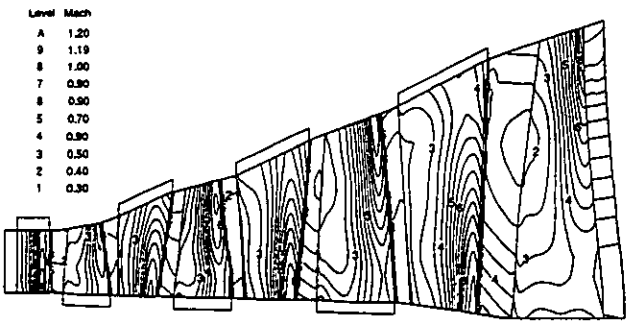

Fig. 12: Computed Mach number distribution

Figure 10 illustrates the streamline pattern through the turbine, obtained from the solution of the stream function equation. As demanded in the cooling air mixing model, the coolant does not influence the direction of the main flow. Contrary to this, the contour plot of the total temperature (Fig. 11) shows the strong influence of the coolant, in terms of total temperature drops in the mixing planes. The tip leakage of the coolant and the cooling air flow through the sealings at hub produce an inhomogeneous distribution of the coolant over the span. This leads to strong temperature gradients in the radial direction.

Figure 12 shows the contour plot of the relative Mach number. The change of the reference frame coincides with the location of the mixing plane. The highest Mach numbers up to Ma=1.22 are located near the hub in the stators due to the blockage of the blades, whereas the peak Mach numbers appear near tip in the rotors due to the high circumferential velocity.

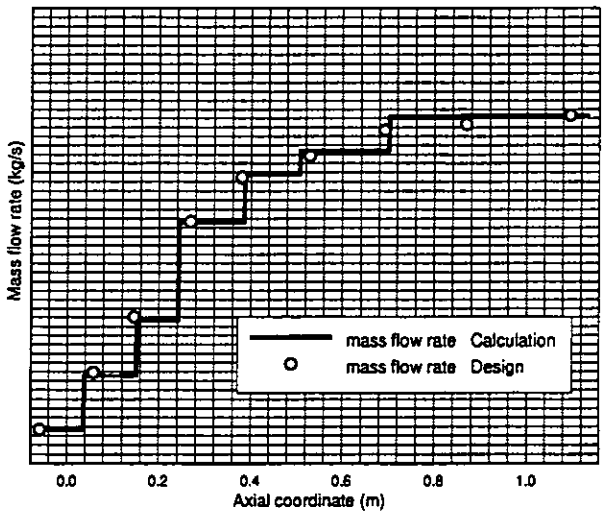

Fig. 13: Computed mass flow rate

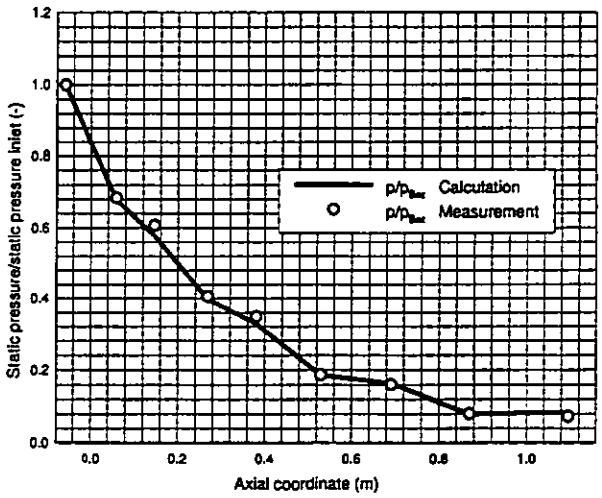

Fig. 14: Static pressure at hub

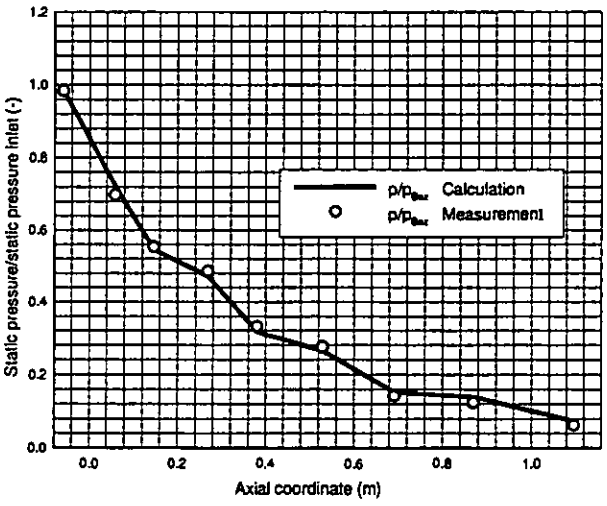

Fig. 15: Static pressure at tip

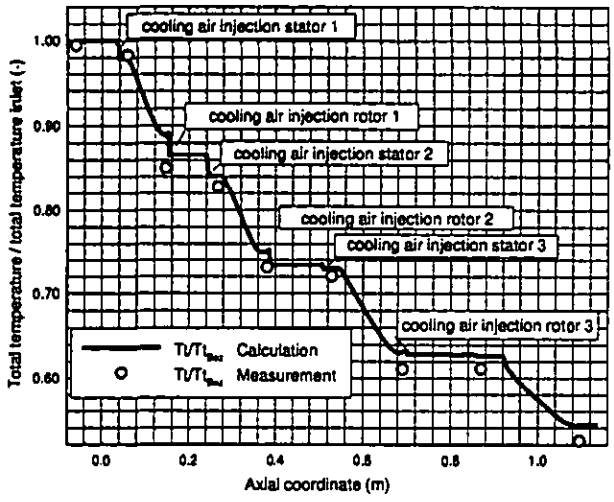

Fig. 16: Total temperature at hub

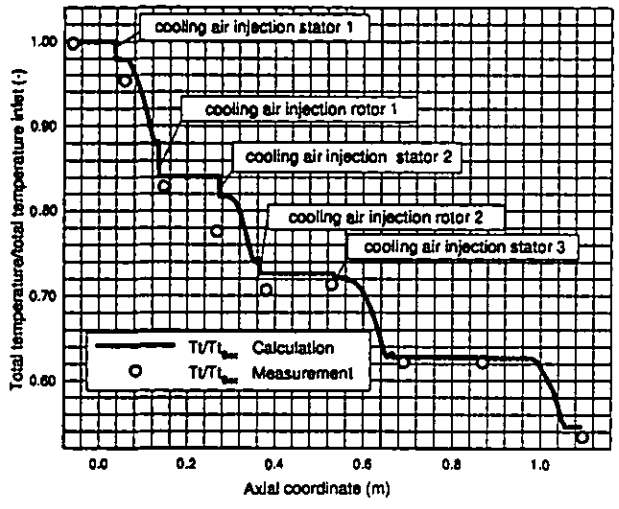

Fig. 17: Total temperature at tip

Figure 13 shows the comparison between calculated and designed mass flux. Due to an agreement with Siemens, Fig. 13 shows only the qualitative development of the mass flux along the flow passage. The highest mass flow rates are ejected in the first four blade rows, while the last ones are less influenced. The obtained numerical results are in good agreement with the design as long as the circumferential averaged peak Mach numbers in the S_{2m}-calculation do not extend a value of about 1.15. Up to this Mach number the artificial density $\tilde{\rho}$ represents the real density in the transonic region in a good manner. Higher peak Mach numbers lead to an increasing numerical dissipation μ and therefore to an increasing difference between the real density and the artificial density $\tilde{\rho}$. This effect causes a small difference between the calculated and the designed mass flux in the end stage of the calculated gas turbine.

Finally, the computed pressure and total temperature distribution are compared with experimental data according to Fig. 14 to Fig. 17. The overall agreement is best for the static pressure distribution, whereas for the total temperature plots some small discrepancies between measurement and computational data are found. A reason for this seems to be the simplicity of the mixing air model. This question still needs to be examined.

CONCLUDING REMARKS

A new analysis method for multistage transonic turbines with coolant mass flow addition has been developed. This procedure combines the advantages of a throughflow method with the advantages of a three dimensional calculation. By replacing the calculation on S_1-planes by a three dimensional inviscid hyperbolic time-dependent algorithm, the iterative coupling of Wu's approach between blade-to-blade planes and hub-to-tip planes can be dropped. Due to the character of the hyperbolic algorithm, transonic flow can be calculated on the S_1-planes without an artificial density model, which can become instable, when choked flow with high Mach numbers occurs. To avoid expensive Navier-Stokes calculations, like in the mixing plane approaches, and to achieve short computation time, the three dimensional algorithm calculate only the inviscid flow field, while the viscous effects and the influence of the cooling air mixing can be considered in the fast stream function algorithm. The circumferential averaging of the flow variables in the S_{2m}-plane leads to smaller peak Mach numbers in the S_{2m}-plane than in the blade-to-blade planes occurs. Therefore the artificial density approach can be used, even when choked flow occurs in the S_1-planes. This method can be applied to machines, whose circumferential averaged peak Mach numbers do not extend Ma=1.15.

This method needed for the calculation of the four stages of the Siemens gas turbine about 20 minutes CPU time on a Siemens/Fujitsu S600 machine.

ACKNOWLEDGEMENTS

The development of this computer code was part of the AG TURBO research program, a cooperational effort between industry, universities and national German research centers. It was financially supported by the German Ministry of Education, Science, Research and Technology (BMBF) under contract No. 0326821.

REFERENCES

Adamczyk, J.J., Celestina, M.L., Beach, T.A., 1990, "Simulation of Viscous Flow Within a Multistage Turbine", Trans. ASME J. of Turbomachinery, Vol. 112

Arnone, A., Benvenuti, E., 1994, "Three-Dimensional Navier-Stokes Analysis of a Two-Stage Gas Turbine", ASME Paper 94-GT-88

Arnone, A., Pacciani, R., 1995, "Rotor-Stator Interaction Analysis Using the Navier-Stokes Equations and a Multigrid Method", ASME Paper 95-GT-177

Benetschik, H., Lohman, A., Lücke, J.R., Gallus, H.E., 1996, "Inviscid and Viscous Analysis of Three-Dimensional Turbomachinery Flows Using an Implicit Upwind Algorithm", AIAA-paper 96-2556

Bohn, D.E., Becker, V.J., Behnke, K.D., Bonhoff B.F., 1995, "Experimental and Numerical Investigations of the Aerodynamic Effects of Coolant Injection through the Trailing Edge of a Guide

Vane", ASME Paper 95-GT-26

Chima, R., 1991, "Viscous Three-Dimensional Calculations of Transonic Fan Performance", 77th Symposium of the Propulsion and Energetics Panel, AGARD

Craig, H.R.M., Cox, H.J.A., 1970, "Performance Estimation of Axial Flow Turbines", Proceedings Institutions of Mechanical Engineers, Vol. 185, 1970/1991

Dawes, W.N., 1990, "Towards Improved Throughflow Capability: The Use of 3D Viscous Flow Solvers in a Multistage Environment", ASME Paper 90-GT-18

Denton, J.D., 1990, "The Calculation of Three Dimensional Viscous Flow Through Multistage Turbines", ASME Paper 90-GT-19

Fan, S., Lakshminarayana,B. 1995, "Time Accurate Euler Simulation of Interaction of Nozzle Wake and Secondary Flow with Rotor Blade in an Axial Turbine Stage Using Nonreflecting Boundary Conditions", ASME Paper 95-GT-230

Hafez, M., Lovell, D., 1981, "Numerical Solution of Transonic Stream Function Equation", AIAA Journal, Vol. 21, No. 3

Hafez, M., South, J., Murmann, E., 1978, "Artificial Compressibility Methods for Numerical Solutions of Transonic Full Potential Equation", AIAA Journal, Vol 17, No. 8

Hah, C., Gallus, H.E., Zeschky, J., 1994, "Endwall and Unsteady Flow Phenomena in an Axial Turbine Stage", ASME Paper 94-GT-143

Harten, A., 1983, "High Resolution Schemes for Hyperbolic Systems of Conservation Laws", Journal of Comp. Physics, Vol. 49

Michelassi, V., Martelli, F., Amecke, J., 1994, "Aerodynamic Performance of a Transonic Turbine Guide Vane With Trailing Edge Coolant Ejection", Part II: Numerical Approach, ASME Paper 94-GT-248

Mildner, F., Gallus, H.E., 1993, "Calculation of Viscous Flow in Turbine Cascades with a Partially-Parabolic Algorithm and Linkage with a Quasi-Three-Dimensional Throughflow Method" AG TURBO report, No. 1.1.2.7

Ni, R.H., Bogoian, J.C., 1989, "Prediction of 3D Multi-Stage Turbine Flow Field Using a Multi-Grid Euler Solver", AIAA Paper 89-0203

Roe, P.L., 1981, "Approximate Riemann Solvers, Parameter Vectors and Difference Schemes", Journal of Computational Physics, Vol. 34, S. 357-372

van Leer, B., 1979, "Towards the Ultimate Conservative Difference Scheme V. a Second-Order Sequel to Godunov's Method", Journal Computational Physics, Vol. 32, S. 101-136

Wu, Chung-Hua, 1951, "A General Through-Flow-Theory of Fluid Flow with Subsonic or Supersonic Velocity in Turbomachines of Arbitrary Hub and Casing Shapes", NACA TN 2302, 1951